Enhanced superconductivity in SnSb under pressure: A first principles study

P V Sreenivasa Reddy and V Kanchana[*]

Department of Physics, Indian Institute of Technology Hyderabad, Kandi, Medak-502 285, Telangana, India.

E-mail: `kanchana@iith.ac.in`

Abstract. First principles electronic structure calculations reveal both SnP and SnSb to be stable in the NaCl structure. In SnSb, a first order phase transition from NaCl to CsCl type structure is observed at around $13\,GPa$, which is also confirmed from enthalpy calculations and agrees well with experimental and other theoretical reports. Calculations of the phonon spectra and hence the electron-phonon coupling, λ_{ep}, and superconducting transition temperature, T_c, at zero pressure for both the compounds and at high pressure for SnSb were performed. These calculations report T_c of $0.614\,K$ and $3.083\,K$ for SnP and SnSb respectively, in the NaCl structure, in good agreement with experiment whilst at the transition pressure, in the CsCl structure, a drastically increased value of T_c around $9.18\,K$ ($9.74\,K$ at $20\,GPa$) is found for SnSb together with a dramatic increase in the electronic density of states at this pressure. The lowest energy acoustic phonon branch in each structure also demonstrate some softening effects, which are well addressed in this work.

Keywords: Phase transition, Fermi surface nesting, Kohn anomaly, Superconductivity

1. Introduction

Understanding the material properties under pressure is always an interesting phenomenon in condensed matter physics, which may cause metal-insulator transitions[1], interband electron transitions[2, 3], Lifshitz transitions[4, 5] etc. Due to this physical properties such as the electronic specific heat, superconducting transition temperature and magnetic behaviours might alter with pressure.

In many 11-type compounds, pressure leads to a phase change from NaCl-type to CsCl-type structure. For instance, in the lanthanide monophosphides LnP (Ln=La, Ce, Pr, Nd, Sm, Gd, Tb, Tm and Yb), the phase change occurs at pressures around 25-50 GPa[6]. In the case of the calcium chalcogenides (CaS, CaSe and CaTe), it is observed at $40\,GPa$, $38\,GPa$ and $33\,GPa$, respectively[7]. A similar transition is also observed in IIIB-nitrides (ScN, YN) and IIIA-nitrides (GaN, InN)[8]. In the case of AgBr, an intermediate KOH-type structure is also observed from 8 to $35\,GPa$[9] between the NaCl-type and CsCl-type structures. Recent theoretical study[10] on similar type of compound, SnAs, reported a phase transition at around 37 GPa from NaCl to CsCl type structure.

SnP was synthesised by Donohue[11] in NaCl and tetragonal structures and was found to be superconducting only in NaCl type structure. The relative phase stability of SnP in NaCl and tetragonal structures is quite unclear[12]. SnSb is useful in energy storage applications[13] and also posses NaCl type structure as ground state and it is observed to undergo a phase change at high pressures from NaCl to CsCl type structure. DFT calculations by Shrivastava $et\ al.$[14] has shed light on the effect of pressure on the electronic structure of SnSb, further demonstrating the structural change that occurs.

It is well known that pressure has a substantial effect on the superconducting properties of elements and compounds[15, 16]. Recently, a high T_c value of 203 K is achieved at a pressure of 200 GPa by Drozdov $et\ al.$[17] in H_2S, highlighting the importance of pressure. In our recent study[10] on SnAs, increase in the T_c and electron phonon coupling is observed under high pressure in the CsCl structure compared to zero pressure NaCl structure. Besides inducing superconductivity, pressure can also enhance the T_c, which motivate us to investigate the effect of pressure on the superconducting properties of SnP and SnSb, a structurally similar compounds to SnAs.

Present manuscript focuses mainly on the ground state, electronic structure, mechanical, vibrational and superconducting properties of investigated compounds. Computational details, which were used to study the above mentioned properties, are given in the following section (section 2). Results and discussions are presented in section 3. Overall conclusions are given in last section (section 4).

2. Computational details

We have used plane wave pseudopotential method (PWSCF) which is implemented in QUANTUM ESPRESSO [18] code for structural and volume optimization of the present

compounds. The same method is also used to get pressure dependent lattice parameter and enthalpy values. The enthalpy values are calculated with $H = E + PV$, where E is the energy of the system at particular pressure(P) and volume (V) in variable-cell relaxation procedure which is inbuilt with in QUANTUM ESPRESSO [18] code. More details on enthalpy calculations can be found in ref[19]. Calculations of band structure, density of states, Fermi surface and elastic constants are performed by using Full-Potential Linearized Augmented Plane Wave (FP-LAPW) method as implemented in WIEN2k [20] code. We have used local density approximation (LDA)[21] for the exchange correlation potential. Throughout the calculations, the R_{MT} (radius of muffin tin spheres) value for each atom was fixed as 2.1 $a.u$, 2.4 $a.u$ and 2.5 $a.u$ for P, Sn and Sb atoms respectively. For the energy convergence, the criterion $R_{MT}*K_{max}$=7 was used, where K_{max} is the plane wave cut-off. The potential and charge density were Fourier expanded up to G_{max}=12 $a.u^{-1}$. All electronic structure calculations are performed with 44×44×44 grid of k points in the Monkhorst-Pack[22] scheme which gives 2168 and 2300 k-points for NaCl and CsCl-type structures respectively in the irreducible part of the Brillouin Zone (BZ). Tetrahedron method [23] was used to integrate the Brillouin zone. Energy convergence up to 10^{-5} Ry is used to get proper convergence of the self consistent calculation. Birch-Murnaghan [24] equation of state was used to fit the total energies as a function of primitive cell volume to obtain the bulk modulus and the equilibrium lattice parameter for the investigated compound. We have checked the effect of spin-orbit coupling (SOC) and have not found any significant changes at the Fermi level with the inclusion of SOC. Further calculations are performed without including SOC.

To compute phonon dispersions and electron-phonon interactions, PWSCF [18] (plane wave self consistent field) method is used. The LDA exchange correlation functional is used in the present calculations for both the compounds. The electron ion interaction is described by using norm-conserving pseudopotentials. The maximum plane wave cut-off energy (ecutwfc) used is 120 Ry and the electronic charge density is expanded up to 480 Ry. A $16 \times 16 \times 16$ k-points grid within the BZ is used for the phonon calculations. Gaussian broadening of 0.005 Ry (dgauss) and a $8 \times 8 \times 8$ uniform grid of q-points are used for phonon calculations.

3. Results and discussions

Total energy calculations are performed to confirm the ground state of SnP and SnSb. From the previous literature ground state of SnP is unclear, and to confirm the same, we have calculated total energy as a function of relative volume in NaCl and tetragonal phases of SnP and are plotted in Fig. 1(a), which reveal the ground state of SnP to be NaCl structure. As discussed above, SnSb crystallize in NaCl structure and might undergo a similar phase change as reported for other compounds with the same structure. From the total energy calculations, as given in Fig. 1(b), SnSb is found to be stable in NaCl structure with lower energy value compared to CsCl structure. Both SnP and

SnSb are having a stable ground state with NaCl-type cubic structure (space group $Fm\bar{3}m$ (No. 225)) with following atomic positions: P/Sb (0.00, 0.00, 0.00) and Sn (0.50, 0.50, 0.50). Again from Fig. 1(b) it is also observed that SnSb might undergo a phase transition from NaCl-type to CsCl-type (space group $Pm\bar{3}m$ (No. 221)) at a compression around V/V_0=0.86. The calculated lattice parameter and bulk modulus values are given in Table 1 for both SnP and SnSb compounds in NaCl-type structure. It is already known that LDA might underestimate the lattice parameter and the same will be overestimated with Generalized Gradient Approximation (GGA). In our case LDA lattice parameter is close to experimental value as given in Table 1 and we further proceeded with rest of the calculations using LDA. Calculated bulk modulus value is around 86 and 63 GPa for SnP and SnSb respectively. For SnP no other reports are available to compare the bulk modulus value, but for SnSb calculated value is more than that observed by Shrivastava et. al[14] and Dabhi et. al[25]. This difference might be due to the usage of different approximations (GGA) for the exchange correlation potential. We have also calculated the change in enthalpy as a function of pressure to compute the exact transition pressure for SnSb and the same is given in Fig. 1(c) and it is observed that the phase transition occurs around 13 GPa, which is a first order phase transition with volume collapse around 6.31%, in good agreement with other theoretical work[14].

Now we move ahead to analyse the electronic structure properties of stable NaCl-type SnP and SnSb at zero pressure. All the electronic structure calculations are performed at the equilibrium lattice parameter. The calculated band structure and atom/orbital projected density of states(DOS) are presented to clarify the characters of the bands and are presented in Fig. 2 and Fig. 3 respectively. The band structure of SnP (Fig. 2(a)) is similar to that found for SnAs[10]. As we move from SnP to SnSb, Fermi level is found to shift towards lower energy region resulting in addition of an extra band crossing the E_F in SnSb (see Fig. 2(b)) compared to SnP, which is having hole nature due to the band crossing from valence band to conduction band. In both the compounds, the band at Γ point is found to posses P/Sb-p character and at L point around 1 eV has Sn-p character. There is a gap in the density of states at around -9.5 eV in SnP and -8.5 eV in SnSb. The peak in the total DOS before the gap is due to 's' states of P/Sb atoms. The peak after the gap is due to 's' states of Sn in both the compounds. There is flat portion in the total DOS before the E_F which is due to 'p' sates of P/Sb atom. At E_F, 'p' sates of P/Sb atom are contributing more to the total DOS. The peak after the E_F is due to 'p' sates of P/Sb atom with admixture of 's' states of Sn atom. The total DOS at Fermi level ($N(E_F)$) is found to be 0.623 and 0.891 $states/eV/f.u$ for SnP and SnSb respectively. We have also observed the covalent nature of bonding between the P/Sb and Sn atoms in this compound. The calculated Sommerfield coefficient (γ) is given in Table 1. along with the experimental value. No other reports are available to compare our calculated γ values.

It is very interesting to know about the Fermi surfaces which has specific importance on the physical properties of a metal through its impact on electron screening. The

calculated Fermi surfaces (FS) at zero pressure is given in Fig. 4(a) for SnP and in Fig. 4(b, c) for SnSb, where we find multiple sheets due to a band crossing E_F at different high symmetry points in both the compounds. An electron pocket at Γ point and sheets near X and K points are observed in both the compounds. From the keen observation of FS, parallel sheets along X-Γ direction are observed in both the compounds resulting in nesting feature along this direction in the present compounds.

To understand the mechanical stability of present compounds at zero pressure, we have calculated the elastic constants and the calculated single and poly crystalline constants are given in Table 2. The calculated single crystalline elastic constants are satisfying the Born's stability criteria, $C_{11} > 0$, $C_{44} > 0$, $C_{11} > C_{12}$, and $C_{11} + 2C_{12} > 0$ indicating the mechanically stable nature of the present compounds at zero pressure. The polycrystalline elastic constants can be calculated from the single crystalline elastic constants using the empirical relations which can be found elsewhere [26, 27, 28, 29]. The calculated Young's modulus (E) is 75.85 and 51.94 GPa for SnP and SnSb respectively. The presence of elastic anisotropy[26] in the present compounds is also confirmed by calculating the anisotropy factor(A). Calculated positive value of Cauchy's pressure $(C_{12} - C_{44})$ indicate the ductile nature of the present compounds, and the same is also confirmed from the calculated Pugh's ratio $(\frac{G_H}{B})$ [30]. The value of Pugh's ratio is less than 0.57 which is known as critical number to separate brittle and ductile nature. The Poisson's [31] ratio (σ) indicate the stability of the crystal against shear and takes value in between -1 to 0.5, where -1 and 0.5 serve as lower and upper bounds respectively. From our calculations, Poisson's ratio value for the present compounds is closer to the upper limit indicating the stiffness of the present compounds. Debye temperature (Θ_D) is one of the important parameter and it determines the thermal characteristics of the materials. The Debye temperature can be obtained from the mean sound velocity, which gives the explicit information about lattice vibration and can be computed directly from $\Theta_D = \frac{h}{k} \left[\frac{3n}{4\pi} \left(\frac{\rho N_A}{M} \right) \right]^{1/3} v_m$. The calculated Debye temperature value for SnSb is in agreement with the earlier theoretical[25] work which is given in the same table.

Now we proceed further with the computation of vibrational properties, which can be used to check the dynamical stability of the present compounds at zero pressure NaCl structure. We have calculated the phonon dispersion curves along different high symmetry directions and the same is given in Fig. 5 along with the phonon density of states (PDOS). The primitive cell of the present compounds have one formula unit with two atoms which gives six phonon branches including three acoustic and three optical branches. The absence of imaginary phonon frequencies indicate the dynamical stability of the present compounds at zero pressure. In SnP, from Fig. 5(a), acoustic and optical modes are well separated due to large difference in atomic masses of Sn and P. From the same plot, major peak in the total PDOS is found near the frequency of 240 cm^{-1} which is due to 'P' atom as shown in the atom projected PDOS. It is also observed that the optical modes are due to the lighter 'P' atom and the remaining acoustic modes are due to the heaver 'Sn' atom. In the case of SnSb, from Fig. 5(b), we observe an interaction of higher frequency acoustic mode with the optical modes along Γ-X, K-Γ,

at L and W points at different frequencies. We also observe degenerate LA2 mode along L-Γ-X and this degeneracy is lifted out in other directions. An anomaly (dip) in the degenerate LA2 mode is observed along Γ-X direction which may have significant effect in the physical properties of SnSb which is not observed in the case of SnP. The same anomaly is observed in the iso-structural SnAs compound[10] and some of the Heusler compounds such as Ni_2MnGa [32], Ni_2MnIn [33], Ni_2MnX (X= Sn, Sb) [34], Ni_2VAl and Ni_2NbX (X=Al, Ga, Sn) [35], which are having same FCC structure. The softening in the acoustic mode leads to Kohn anomaly, which is due to the interaction of electronic states with phonon at the E_F together with parallel sheets in the FS topology. In SnSb also this interaction might be a reason for the anomaly. To check the atomic contribution for this phonon plot, we have calculated total PDOS and are plotted in Fig. 5(b). From this figure, major peak in the total PDOS observed around 120 cm^{-1} is due to both Sn and Sb atoms, which are having almost equal contribution (which is due to the nearly same atomic mass) around this frequency range (see Fig. 5(d)).

Having determined the phonon structure as discussed above, the electron-phonon coupling can be calculated to explore the superconducting properties. As discussed in section 1, present compounds are found to have superconducting nature in NaCl structure which is the ground state. The electron phonon coupling constant (λ_{ep}) is extracted from the Eliashberg function ($\alpha^2F(\omega)$) which can be used to determine the superconducting transition temperature (T_c) of a conventional phonon mediated superconductor. The T_c of the present compound is calculated by using Allen-Dynes [36] formula, $T_c = \frac{\omega_{ln}}{1.2}exp(-\frac{1.04(1+\lambda_{ep})}{\lambda_{ep}-\mu^*(1+0.62\lambda_{ep})})$, where ω_{ln} is logarithmically averaged phonon frequency, λ_{ep} is electron phonon coupling constant and μ^* is Coulomb pseudopotential. The representation of $\alpha^2F(\omega)$ is $\alpha^2F(\omega) = \frac{1}{2\pi N(\epsilon_f)} \sum_{qj} \frac{\nu_{qj}}{\hbar\omega_{qj}}\delta(\omega - \omega_{qj})$. This function is often very similar to the phonon DOS ($F(\omega) = \sum_{qj} \delta(\omega - \omega_{qj})$) and differs from the phonon DOS by having a weight factor $1/2\pi N(\epsilon_f)$ inside the summation. In the above formula $N(\epsilon_f)$ is the electronic density of states at the E_F and ν_{qj} is the phonon line width which can be represented as $\nu_{qj} = 2\pi\omega_{qj} \sum_{knm} |g^{qj}_{(k+q)m,kn}|^2\delta(\varepsilon_{kn} - \varepsilon_F)\delta(\varepsilon_{(k+q)m} - \varepsilon_F)$, where Dirac delta function express the energy conservation conditions and g is the electron phonon matrix element. λ_{ep} can be expressed in terms of $\alpha^2F(\omega)$ as $\lambda_{ep} = 2 \int \frac{d\omega}{\omega}\alpha^2F(\omega) = \int \lambda(\omega)d\omega$, where $\lambda(\omega) = \frac{2\alpha^2F(\omega)}{\omega}$. The calculated Eliashberg function is plotted in Fig. 5(a) and 6(b) for SnP and SnSb respectively, where we find peaks at frequency around 220, 230 cm^{-1} in SnP and around 120, 70 cm^{-1} in SnSb. The height of the peak indicate the high phonon linewidth and high electron phonon coupling constant at that frequency region and is found to decrease gradually to lower frequencies. The calculated T_c values of the investigated compounds are 0.614 and 3.083 K with a value of λ_{ep} around 0.41 and 0.68 for SnP and SnSb respectively by considering the μ^* value to be 0.13. These calculated values are in good agreement with the other reported values[25] and are given in Table 3. In addition, we have calculated phonon linewidth for all phonon modes along high symmetry directions for both SnP and SnSb at zero pressure and are given in Fig. 7(a) and 7(b). We find the optical phonon modes to contribute more for the electron phonon coupling as compared to acoustic phonon

modes in both the compounds which is already confirmed from Eliashberg function plot.

From the above discussions superconducting nature is confirmed in both the compounds at zero pressure NaCl structure. From the calculated total energy and enthalpy calculations (as discussed from Fig. 1) phase transition is observed only in SnSb from NaCl to CsCl-type structure. So, it is quite reasonable to study the pressure effect on the above mentioned properties of SnSb which are presented in next section.

3.1. Pressure effect on SnSb

As we already discussed above, from the enthalpy calculations, SnSb undergoes a phase transition from NaCl to CsCl structure at around 13 GPa. We have calculated the band structure of NaCl-type and CsCl-type structures at transition pressure (13 GPa) and are given in Fig. 2(c) and 2(d). As pressure increases widening of valence band region is observed in NaCl-type structure together with the band shifting at Γ point. As pressure increases from 0 to 13 GPa, the band at Γ point is shifted towards the E_F, resulting in decrease of Sb-p character with pressure. Due to this, the occupied area of the band which cross the E_F at Γ point is decreased which might have an effect on the size of electron pocket at the Γ point in the FS. At the transition, around 13 GPa, lattice parameter for CsCl-type structure is found to be 3.548 $\mathring{A}$. The band structure scenario of CsCl-type structure is completely different in comparison with NaCl-type structure (see Fig. 2(d)). In CsCl-type structure, six bands are found to cross at E_F, whereas in NaCl-type structure it is only two which implies the significant change on the FS topology in CsCl-type compared to NaCl-type structure. Upto a pressure of 20 GPa we have not found any change in the band structure topology in CsCl-type SnSb, and hence no change in FS is observed.

Calculated FS for NaCl-type at 13 GPa is given in Fig. 4(d, e), where we can see the decrease in the size of the electron pocket at Γ point (Fig. 4(e)) which is due to the band shifting at this pressure. At the same pressure, FS topology of CsCl-type is given in Fig. 6 along with the corresponding Brillouin zone. From this figure, we have observed six FS corresponding to six bands crossing the E_F, which is evident from band structure plots in Fig. 2(d) and might lead to drastic changes in T_c. Among these six FS's, third one (Fig. 6(c)) has parallel sheets around M point, along R-M, X-M and Γ-M. Beyond this pressure no FS topology change is observed in CsCl-type upto the final pressure (studied up to 20 GPa).

Calculated total electronic density of states as a function of pressure is given in Fig. 3(c), As pressure increases, the total DOS in both the structures is found to decrease monotonically. At the transition pressure total density of states is found to be increased by around 12% compared to zero pressure structure, which certainly might alter the T_c in CsCl structure.

To check the mechanical stability of CsCl-type SnSb at transition pressure we have calculated the single and poly crystalline elastic constants at 13 GPa and are given in Table 2. These values are satisfying the mechanical stability criteria at this pressure

indicating the stable nature of CsCl-type structure at this pressure. The calculated bulk modulus is found to be 113 GPa which is large compared to the zero pressure NaCl-type structure. The calculated single crystalline elastic constants as a function of pressure is plotted in Fig. 8(a) for both NaCl and CsCl-type SnSb, where we can observe C_{11} and C_{12} to be more sensitive to pressure compared to C_{44}. We have also observed the decrease in the value of C_{11} and increase in C_{12} and C_{44} in CsCl-type structure when compared to NaCl-type structure at transition pressure. From the same figure, non-monotonic variation in C_{11}, C_{12} and C_{44} is observed in CsCl-type structure with increase in pressure upto 20 GPa. This non-monotonic behaviour may further lead to changes in the other physical properties in the CsCl-type SnSb under pressure.

Pressure effect on the vibrational properties is always an interesting phenomenon which can be used to understand the dynamical behaviour of the system under the application of pressure. We have calculated phonon dispersion curves at transition pressure for both the phases of SnSb. For NaCl-type at the transition pressure (red colour dotted line) softening in the lower acoustic mode is observed near Γ, X and K high symmetry points as shown in Fig. 5(b). There are some interesting features in the dispersions that alter both between the two structures and with the application of pressure. In the NaCl structure, there is a degeneracy in the LA2 mode along L-Γ-X which is lifted out in other directions but the same degeneracy still remain through the application of pressure. The calculated phonon dispersion for CsCl-type SnSb at the transition pressure is given in Fig. 5(c), where we have observed a similar degeneracy in the CsCl structure along the Γ-X direction that still remains under pressure. An interaction of the higher frequency acoustic modes with the optical modes is seen at various points in the BZ for both structures. In the NaCl structure, pressure acts to lift this interaction quite considerably, pulling apart the acoustic and optical modes whilst in the CsCl structure the application of further pressure has little effect on the interplay between the acoustic and optical branches.

The calculated Eliashberg function is found to decrease at 13 GPa compared to zero pressure in NaCl-type SnSb indicating the decrease in the electron-phonon coupling constant at this pressure compared to zero pressure which may further lead to decrease in the T_c for the NaCl-type structure at this pressure. From Fig. 5(c), we have observed overlapping of acoustic and optical modes at different high symmetry directions. Phonon softening around 'M' high symmetry point is observed in CsCl-type SnSb. From the Eliashberg function plotted in Fig. 5(b) and 5(c), it can be seen that the T_c of CsCl type SnSb would be higher. In addition, we have calculated the phonon linewidth plots (which is proportional to λ_{ep}) for all the modes and are plotted in Fig. 7(d) for 13 GPa and in Fig. 7(e) for 20 GPa respectively along high symmetry directions. From the plots we could observe the optical modes to contribute more towards λ_{ep} than the acoustic modes. Though we observe a peak around the frequency region corresponding to the phonon softening around 'M' point, the major peak in the Eliashberg function arises from the optical modes, which is further confirmed from the phonon linewidth.

At the transition pressure (13 GPa), when we compared phonon dispersion plots

for both NaCl and CsCl structures, frequency of higher optical modes decreased in CsCl-type structure compared to NaCl-type structure. In addition, a softening nature is observed in CsCl-type near Γ point along Γ-M. In the same way maximum peak in the total PDOS is observed at high frequency optical region in NaCl-type and the same peak is found to be broadened in CsCl-type. In NaCl-type, total PDOS corresponding to acoustic modes is found to be flat but the same in CsCl-type is found to have multiple peaks. As pressure increases up to 20 GPa we have observed hardening in the frequencies of all modes in CsCl-type.

To check the superconducting nature in CsCl phase we have calculated the superconducting properties of CsCl-type SnSb at transition pressure (13 GPa). Surprisingly we have observed high T_c value in the CsCl-type structure around 9.18 K with higher λ_{ep} of 1.55. These values are also given Table 3. The reason may be due to the increase in the total electronic DOS in CsCl-type when compared to NaCl-type which will lead to increase the probability of electron-phonon interaction which again may be a reason for the increase in the λ_{ep} and T_c in CsCl-type compared to NaCl-type. We have also calculated the variation of T_c, λ_{ep} and ω_{ln} with pressure for both NaCl and CsCl-type and are plotted in Fig. 8(b). As pressure increases T_c and λ_{ep} decreases monotonically in NaCl-type but in CsCl-type it is found to have non-monotonic variation with pressure. Eventhough we have not observed any non-monotonic variation in total electronic DOS and change in FS topology with increasing pressure in CsCl-type, but observed non-monotonic variation in λ_{ep} and T_c. This behaviour may be mainly phonon driven and may not be electron driven in the CsCl-type SnSb which is similar to CsCl-type SnAs[10]. It is also found that T_c follows ω_{ln} behaviour in CsCl-type but the same is not observed in NaCl-type. From the present work, CsCl phase is found to have higher T_c and λ_{ep} values compared to NaCl-type indicating the strong coupling nature in CsCl phase.

4. Conclusions

Density functional calculations are performed for both SnP and SnSb compounds which confirm the stable NaCl ground state in both the compounds. Fermi surface nesting feature is observed in both the compounds at zero pressure. Phase transition from NaCl to CsCl-type structure is observed at around 13 GPa (V/V$_0$=0.86) in SnSb. At the transition pressure, change in the band structure and FS topology is observed in NaCl-phase together with a softening in the acoustic mode in NaCl type SnSb and the same softening nature in the CsCl-type SnSb is also observed in the acoustic mode at the same transition pressure. Sudden drop in the T_c and λ_{ep} is observed in NaCl-type with increasing pressure. At the transition pressure two fold increase in the T_c (T_c of 9.18 K) is observed in CsCl phase with high λ_{ep} of 1.55 indicating strongly coupled superconducting nature in CsCl phase which needs to be verified experimentally.

5. Acknowledgement

[1] Mcmahan A K 1986 *Physica B* **139/140** 31

[2] Tups H, Takemura K and Syassen K 1982 *Phys. Rev. Lett.* **49** 177

[3] Jayaraman A, in "Handbook on the Physics and Chemistry of Rare Earths", edited by K. A. Gschneidner Jr and L. Eyring, (North Holland, Amsterdam, 1979) Vol 2 p. 575.

[4] Garg A B, Godwal B K, Meenakshi S, Modak P, Rao R S, Sikka S K, Vijay Kumar V, Lausi A and Bussetto E 2002 *J. Phys.:Condens. Matter* *14* 10605

[5] Chandrashekar N V, Rajagopalan M, Meng J F, Polvani D A and Badding J V 2005 *J. Alloys Comp.* **388** 215

[6] Takafumi Adachi, Ichimin Shirotani, Junichi Hayashi and Osamu Shimomura 1998 *Physics Letters A* **250** 389-393

[7] Huan Luo, Raymond G. Greene, kouros Ghandehari, Ting Li and Arthur L. ruoff 1994 *Phy. Rev. B* **50** 232-237

[8] Luis Mancera, Jairo A. Rodriguez and Noboru Takeuchi 2004 *Phys. Stat. Sol. (b)* **241** 2424-2428

[9] Jochym P T and Parlinski K 2001 *Phys. Rev. B* **65** 024106

[10] Sreenivasa Reddy P V, Kanchana V, Millichamp T E, Vaitheeswaran G and Dugdale S B 2017 *Physica B* **505** 33-40

[11] Donohue P C 1970 *Inorganic Chemistry* **9** 335-337

[12] Carl W F T Pistorius 1976 *Progress in Solid State Chemistry* **11** 1-151

[13] Zhufeng Hou, Aiyu Li, Zizhong Zhu, Meichun Hung and Yong Yang 2004 *J. Mater. Sci. Technol.* **20** 743-745

[14] Deepika Shrivastava, Shweta D. Dabhi, Prafulla K. Jha and Sankar P. Sanyal 2016 *Solid State Communications* **243** 16-22

[15] Narlikar A V 2014 "Superconductors", Oxford University Press, ISBN:9780199584116, page no. 98

[16] Hirsch J E and Hamlin J J 2010 *Physica C* **470** S937-S939

[17] Drozdov A P, Eremets M I, Troyan I A, Ksenofontov V, Shylin S I 2015 *Nature* **525** 73-76

[18] Giannozzi P, Baroni S, Bonini N, Calandra M, Car R, Cavazzoni C, Ceresoli D, Chiarotti G L, Cococcioni M, Dabo I, Corso A D, de Gironcoli S, Fabris S, Fratesi G, Gebauer R, Gerstmann U, Gougoussis C, Kokalj A, Lazzeri M, Martin-Samos L, Marzari N, Mauri F, Mazzarello R, Paolini S, Pasquarello A, Paulatto L, Sbraccia C, Scandolo S, Sclauzero G, Seitsonen A P, Smogunov A, Umari P and Wentzcovitch R M 2009 *J. Phys.: Condens. Matter* **21** 395502

[19] Vaitheeswaran G, Kanchana V, Rajagopalan M 2002 *J. alloys. compd.* **336** 4655

[20] Blaha P, Scwarz K, Sorantin P and Tricky S B 1990 *Comput. Phys. Commun.* **59** 399-415

[21] Ceperley D M and Alder B J 1980 *Phys. Rev. Lett.* **45** 566

[22] Monkhorst H J and Pack J D 1976 *Phys. Rev. B* **13** 5188

[23] Blöchl P, Jepsen O and Andersen O K 1994 *Phys. Rev. B* **49** 16223

[24] Birch F 1947 *Phys. Rev.* **71** 809

[25] Shweta D. Dabhi, Deepika Shrivastava, Prafulla K. Jha and Sankar P. Sanyal 2016 *Physica C* **528** 56-59

[26] Kanchana V 2009 *Euro. Phys. Lett.* **87** 26006

[27] Kanchana V, Vaitheeswaran G, Ma Yanming, Xie Yu, Svane A and Eriksson O 2009 *Phys. Rev. B* **80** 125108

[28] Kanchana V, Vaitheeswaran G, Svane A and Delin A 2006 *J. Phys.: Condens. Matter* **18** 9615

[29] Kanchana V, Vaitheeswaran G and Svane A 2008 *J. Alloy. Comp.* **455** 480

[30] Pugh S F 1954 *Philos. Mag.* **45** 823

[31] Wortman J J, Evans R A 1965 *J. App. Phy.* **36** 153

[32] Bungaro C, Rabe K M and Dal Carso A 2003 *Phys. Rev. B* **68** 134104

[33] Ağduk S and Gökoğlu G 2011 *Euro. Phys. J. B* **79** 509-514

[34] Ağduk S and Gökoğlu G 2012 *J. Alloy. Comp.* **511** 9-13

[35] Sreenivasa Reddy P V, Kanchana V, Vaitheeswaran G and David J Singh 2016 *J. Phys.: Condens. Matter.* **28** 115703

[36] Allen P B and Dynes R C 1987 *J. Phys. C: Solid State Phys.* **8** L158

[37] Marris W Jones and Brown E G 1930 *Nature* **126** 846-847

Table 1. Calculated lattice parameter (a) in $\mathring{A}$, bulk modulus (B) in GPa, total density of states ($N(E_F)$) in $states/eV/f.u$ and Sommerfield coefficient (γ) in the units of $mJ/molK^2$ for SnP at zero pressure and SnSb at zero pressure and at the transition pressure compared with other values.

Parameters	Calculated	Experimental	other theory
SnP NaCl-type			
a	5.489	5.5359[11]	
B	86		
$N(E_F)$	0.623		
γ	1.47		
SnSb NaCl-type			
a	6.050	6.092[37]	6.1807[14],6.173[25]
B	63		52.7[14], 53.1[25]
$N(E_F)$	0.891		0.95[14], 1.04[25]
γ	2.10		
SnSb CsCl-type			
a	3.548		3.7937[14]
B	113		53.8[14]
$N(E_F)$	1.017	-	
γ	2.40		

Table 2. Calculated single crystalline elastic constants and mechanical properties of SnP and SnSb at zero pressure NaCl-type structure and SnSb in CsCl-type structure at transition pressure. Where B is bulk modulus, E is Young's modulus, A is Anisotropy factor, CP is Cauchy's pressure, σ is Poisson's ratio, G_H is Voigt-Reuss-Hill modulus, v_l, v_t, v_m are the longitudinal, transverse and mean sound velocities respectively and Θ_D is Debye temperature. Other values are given in brackets

Parameters	SnP(NaCl-type)	SnSb (NaCl-type)	SnSb (CsCl-type at 13 GPa)
C_{11} (GPa)	112.96	86.44	159.36
C_{12} (GPa)	72.85	51.60	89.88
C_{44} (GPa)	35.07	20.23	59.73
B (GPa)	86.21	63.22	113.03
E (GPa)	75.85	51.94	126.28
A	1.75	1.16	1.72
CP ($C_{12} - C_{44}$)	37.78	31.37	30.15
Pugh's ratio	0.32	0.30	0.42
σ	0.35	0.36	0.31
v_l (km/s)	9.06	7.01	11.56
v_t (km/s)	4.32	3.25	6.02
v_m (km/s)	4.86	3.66	6.74
Θ_D (K)	332	227(213[25])	377

Table 3. Superconducting properties of SnP at zero pressure NaCl-type structure, SnSb at zero pressure and at the transition pressure (13 GPa) in CsCl-type structure. Other values are given in brackets.

Parameters	SnP (NaCl-type)	SnSb NaCl-type at zero pressure	SnSb (CsCl-type at 13 GPa)
T_c (K)	0.614	3.083 (3.1[25])	9.18 (9.74 at 20 GPa)
λ_{ep}	0.41	0.68(0.70[25])	1.55 (1.21 at 20 GPa)
ω_{ln}	242.97	124.75	84.88(121.81 at 20 GPa)

(a)

(b)

(c)
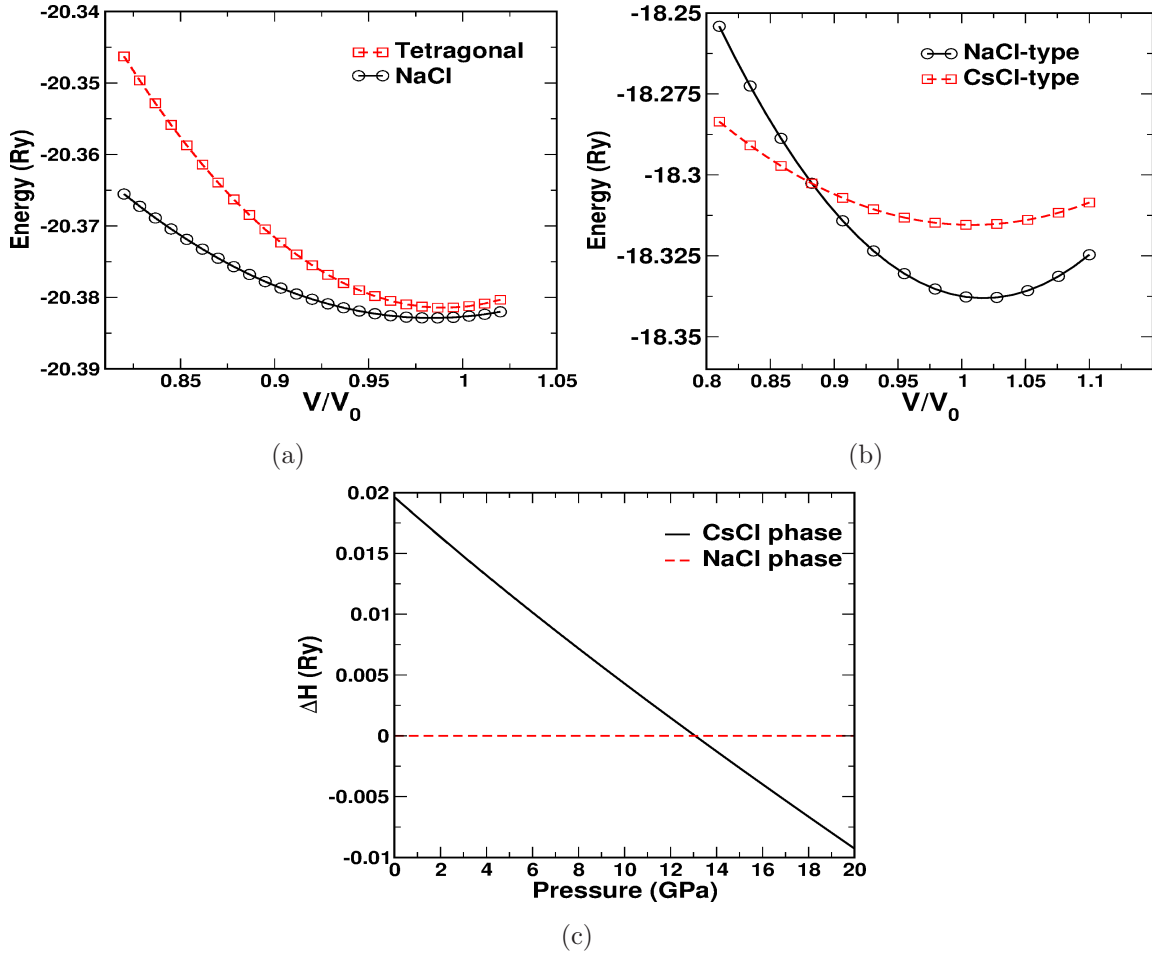
Figure 1. Total energy as a function of V/V$_0$ for (a) SnP where circle and square symbols represent NaCl and tetragonal phases respectively, (b) SnSb where circle and square symbols represent NaCl and CsCl phases respectively. (c) Change in enthalpy during phase change from NaCl to CsCl type at the pressure of 13 GPa in SnSb(colour online).
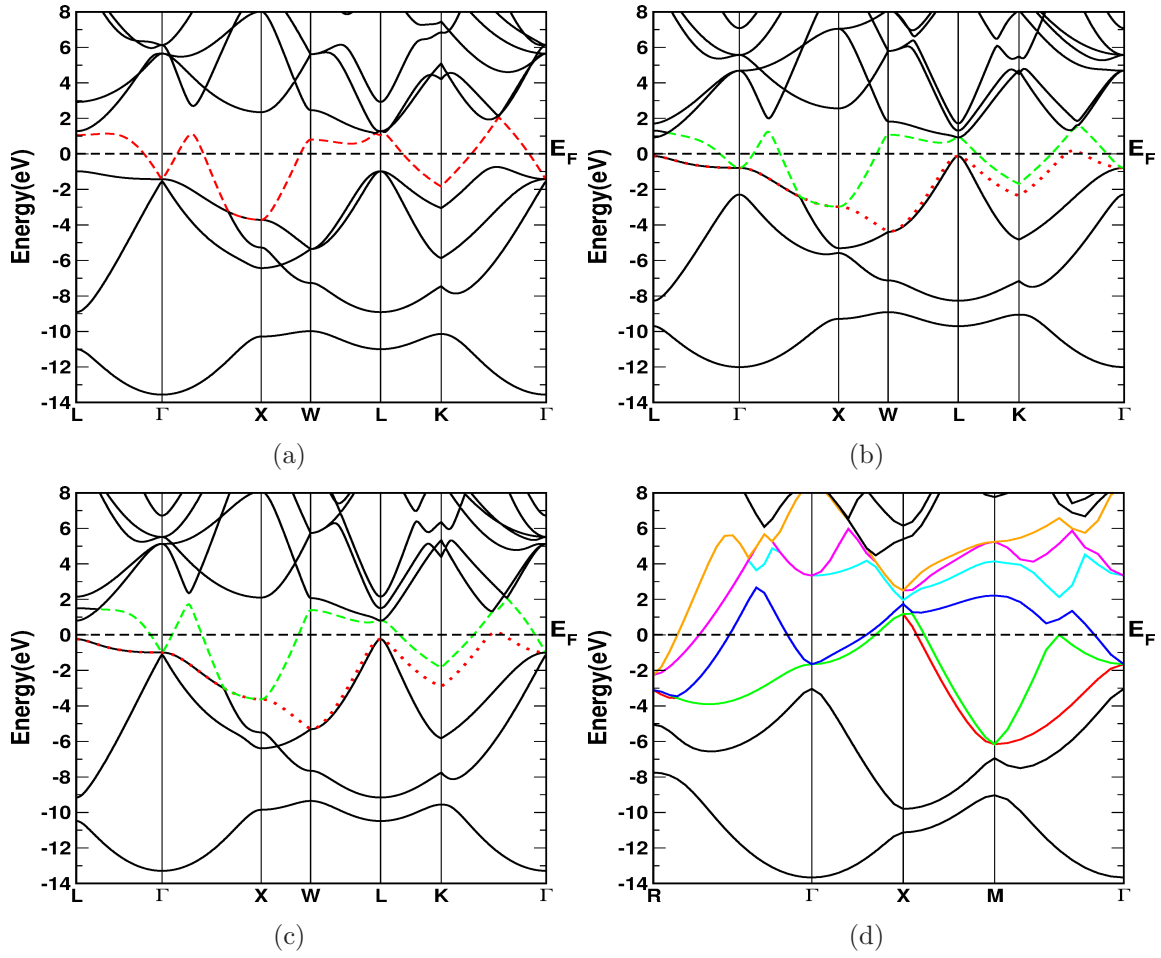
Figure 2. (a) Band structure for SnP at zero pressure, (b) Band structure for SnSb at zero pressure and (c) at transition pressure (13 GPa) in NaCl-phase. (d) Band structure for SnSb in CsCl-type at transition pressure (13 GPa)(colour online).
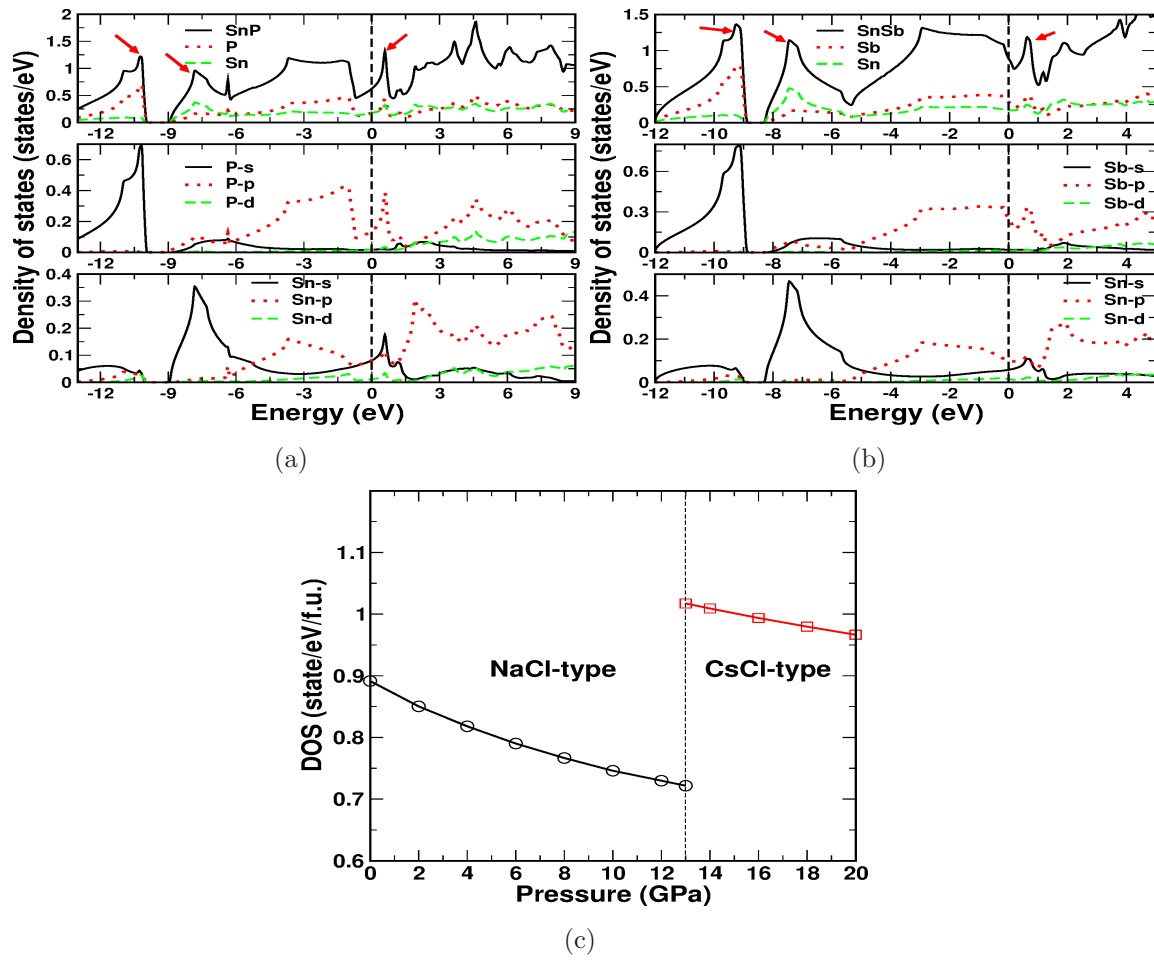
Figure 3. Total and atom projected density of states (a)at zero pressure for SnP, (b) at zero pressure for SnSb in NaCl-type and (c) variation of total density of states with pressure in SnSb(colour online).
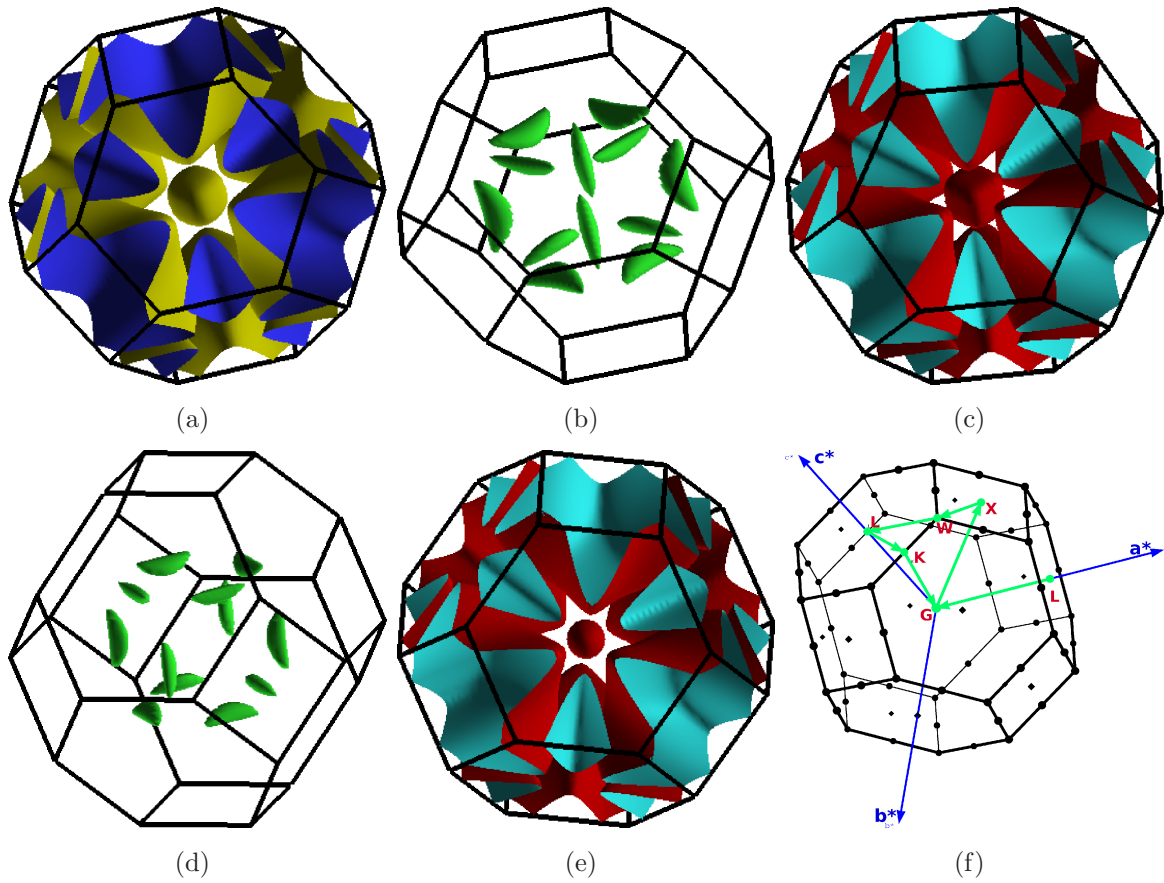
Figure 4. (a) Fermi surface for SnP at zero pressure. Fermi surface of SnSb (b, c) at zero pressure and (d, e) at transition pressure (13 GPa). (f) Brillouin zone with high symmetry points for NaCl-type structure(colour online).
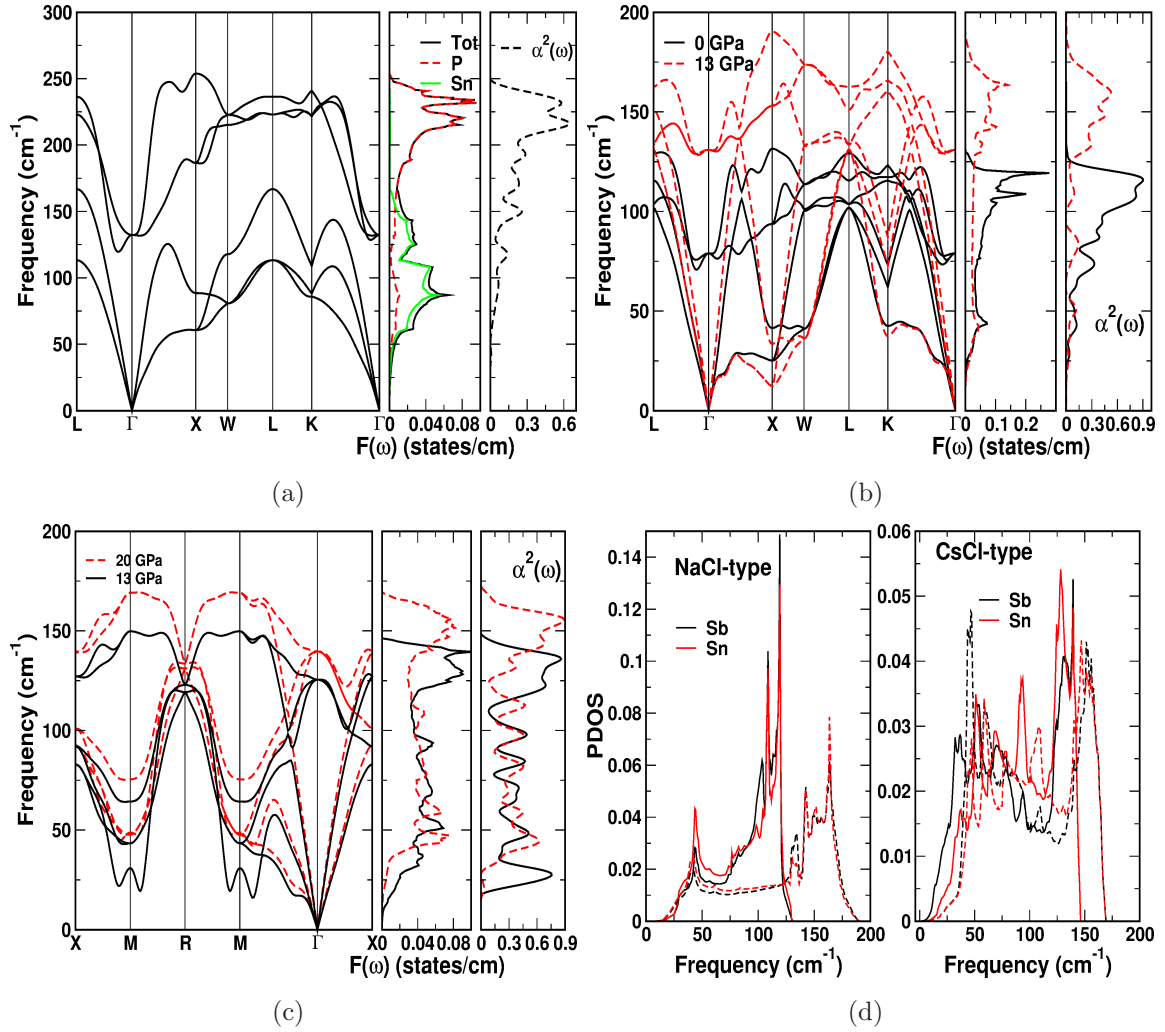
Figure 5. (a)Phonon dispersion along with total phonon density of states and Eliashberg function for SnP in NaCl phase at zero pressure. (b) Phonon dispersion along with total phonon density of states and Eliashberg function for SnSb in NaCl-phase at 0 and 13 GPa. (c) Phonon dispersion along with total phonon density of states and Eliashberg function for SnSb in CsCl-phase at 13 and 20 GPa, (d) Atom projected phonon density of states for NaCl phase at zero pressure (solid lines) and 13 GPa (dotted lines) and CsCl phase at 13 (solid lines) and 20 GPa (dotted lines)(colour online).
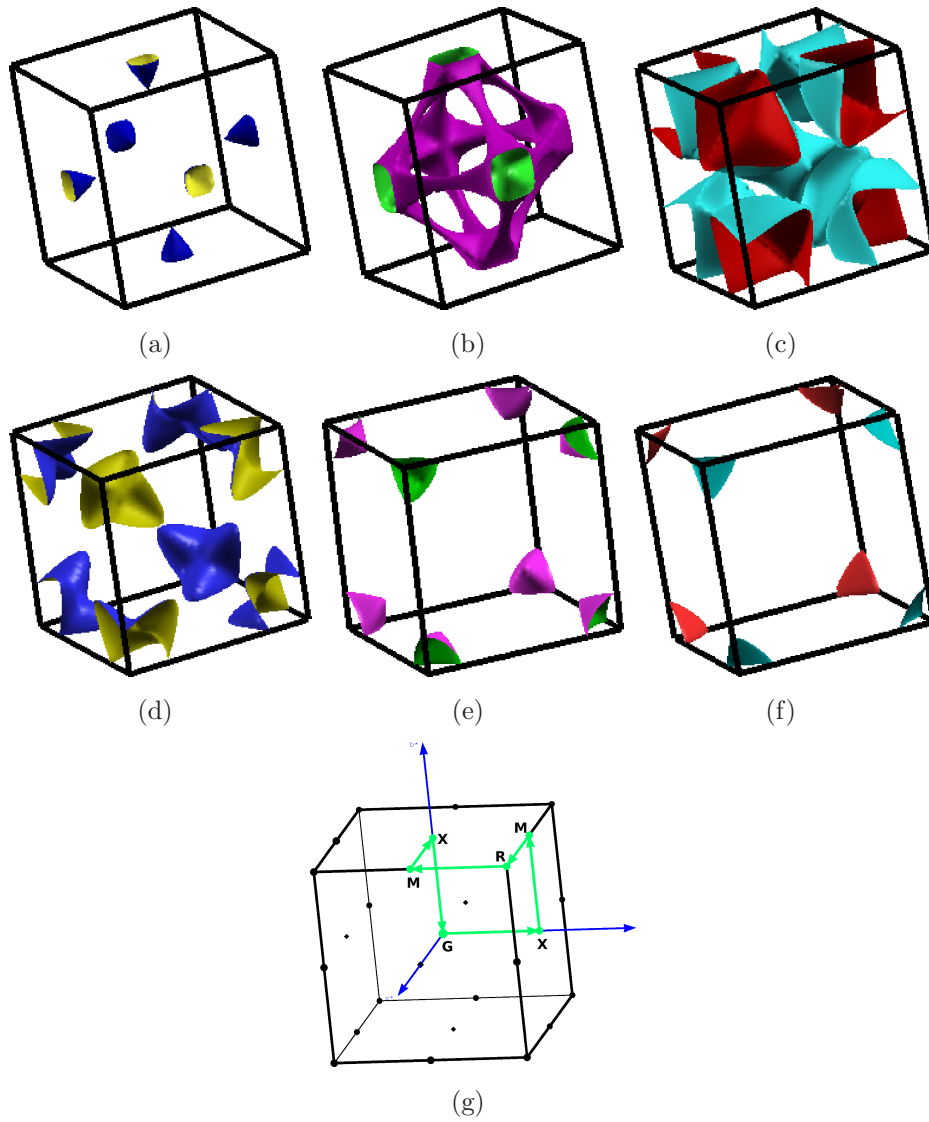
Figure 6. Fermi surface for CsCl-type SnSb at transition pressure (13 GPa)(a) for band no. 13, (b)for band no. 14, (c) for band no. 15, (d)for band no. 16, (e)for band no. 17, (f)for band no. 18 and (g) brillouin zone for CsCl-type(colour online).
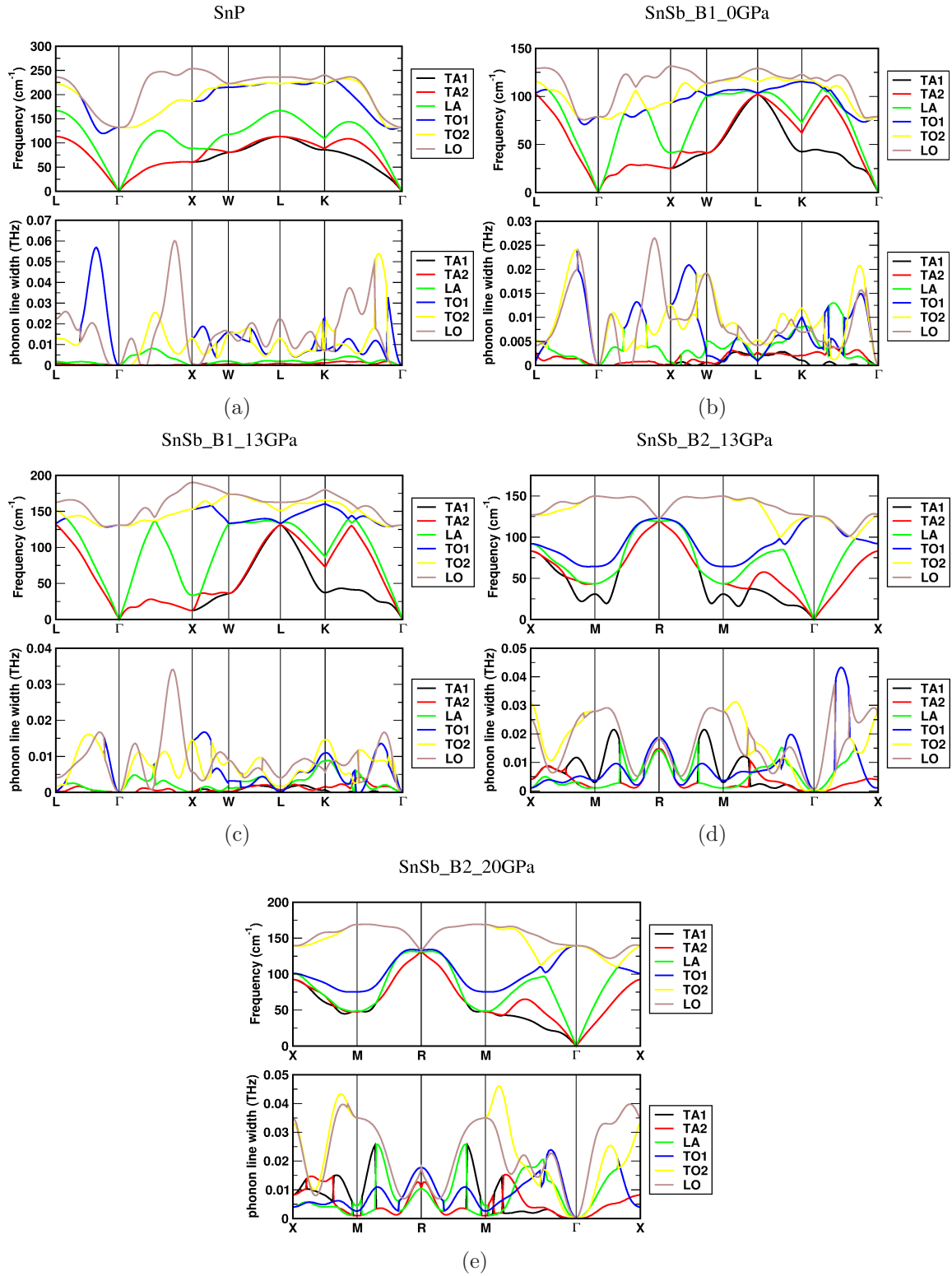
Figure 7. Phonon linewidth along with phonon dispersion plots for (a)SnP, (b) NaCl type SnSb at zero pressure, (c) NaCl type SnSb at 13 GPa, (d)CsCl type SnSb at 13 GPa and (e)CsCl type SnSb at 20 GPa(colour online).
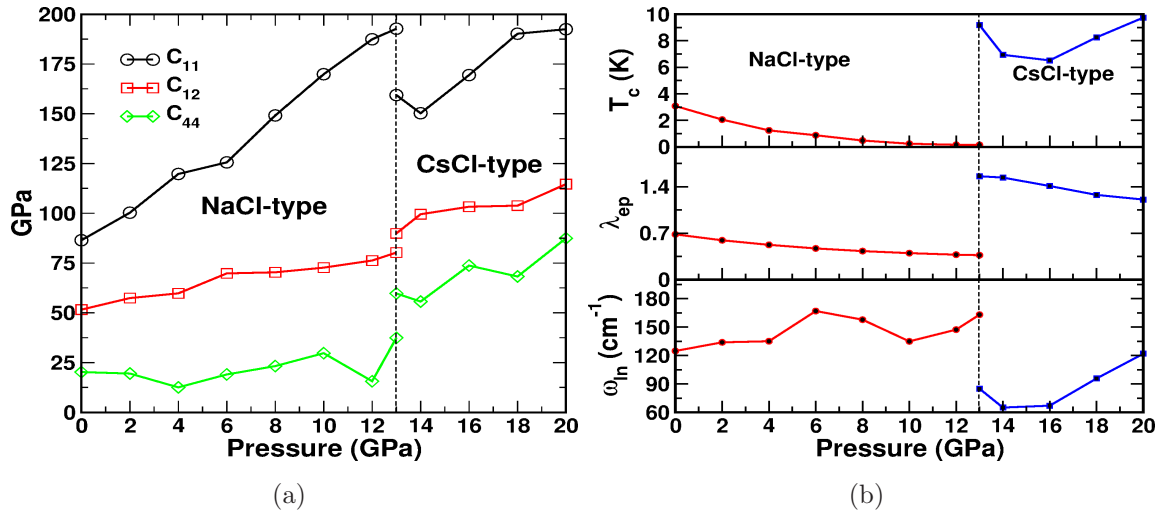
Figure 8. (a)Elastic constants as a function of pressure for SnSb. (b) Pressure dependence of T_c, λ_{ep} and ω_{ln} for NaCl-type up to 13 GPa and CsCl-type above 13 GPa for SnSb(colour online).